

THE COMPOSITION OF GOLD IN THE CERRO CASALE GOLD-RICH PORPHYRY DEPOSIT, MARICUNGA BELT, NORTHERN CHILE

CARLOS PALACIOS[§]

Department of Geology, Universidad de Chile, P.O. Box 13518, (21) Santiago, Chile

GÉRARD HÉRAIL

IRD, 209-213 rue La Fayette, F-75480 Paris, Cedex 10, France

BRIAN TOWNLEY, VÍCTOR MAKSAEV AND FABIÁN SEPÚLVEDA

Department of Geology, Universidad de Chile, P.O. Box 13518, (21) Santiago, Chile

PHILIPPE de PARSEVAL

Laboratoire de Minéralogie, UMR 5563, Université Paul Sabatier, 39, Allées Jules-Guesde, F-31000 Toulouse, France

PABLO RIVAS, ALFREDO LAHSEN AND MIGUEL ANGEL PARADA

Department of Geology, Universidad de Chile, P.O. Box 13518, (21) Santiago, Chile

ABSTRACT

The Cerro Casale gold-rich orebody, located in the Maricunga Belt, in northern Chile, is a Miocene deposit hosted in diorite and granodiorite porphyries. Two broad types of hypogene alteration are associated with gold mineralization: potassic and white mica. The geochemical study of gold crystals involved the electron-microprobe analysis of 176 gold grains from 29 samples. These samples were collected from diamond drill-cores at various depths. The gold crystals deposited during potassic alteration have high abundances of Ag (8 to 28 wt.%) and low concentrations of Cu (n.d. to 0.24 wt.%). However, gold crystals deposited during white mica alteration have low concentrations of Ag (1 to 9 wt.%) and higher abundances of Cu (0.06 to 0.34 wt.%). In addition, gold crystals recovered from fragments of both porphyries included in a white mica hydrothermal breccia apparently maintain their original Ag and Cu concentrations.

Keywords: gold-rich porphyry copper, gold crystals, geochemistry, Maricunga Belt, Chile.

SOMMAIRE

Le gisement aurifère de Cerro Casale, d'âge miocène, situé dans la ceinture de Maricunga, dans le nord du Chili, a un encaissant de porphyre dioritique ou granodioritique. Deux genres d'altération hypogène sont associés à la minéralisation, potassique et à mica blanc. L'étude géochimique des cristaux d'or, faite par analyses à la microsonde électronique, a porté sur 176 grains prélevés de 29 échantillons. Ceux-ci proviennent de carottes à diverses profondeurs. L'or déposé au cours de l'altération potassique contient une teneur élevée en argent (de 8 à 28%, poids) et une faible teneur en cuivre (en dessous du seuil de détection jusqu'à 0.24%). Toutefois, les cristaux déposés au cours de l'altération menant à un mica blanc contiennent beaucoup moins d'argent (entre 1 et 9%) et plus de cuivre (de 0.06 à 0.34%). De plus, les cristaux d'or récupérés des blocs des deux sortes de porphyre inclus dans la matrice riche en mica blanc d'une brèche hydrothermale semblent conserver leurs proportions originales de Ag et de Cu.

(Traduit par la Rédaction)

Mots-clés: gisement de type porphyre aurifère, cristaux d'or, géochimie, ceinture de Maricunga, Chili.

[§] *E-mail address:* cpalacio@cec.uchile.cl

INTRODUCTION

The Maricunga Belt (Vila & Sillitoe 1991) is located between latitudes 26° and 28°S in the Andean Cordillera, at altitudes ranging from 4,000 to 5,000 m above sea level (Fig. 1). The Belt comprises gold-rich porphyry and precious-metal epithermal mineralization, formed during late Oligocene and Miocene hydrothermal events (Sillitoe *et al.* 1991). The ore deposits hosted in the Maricunga Belt contain resources totalling more than 1.42×10^6 kg of gold and approximately 12.76×10^6 kg of silver, and other prospects under exploration will likely increase this potential. The Cerro Casale porphyry gold deposit consists of a mineralized subvolcanic stock

and hydrothermal breccia complex of middle Miocene age, located in the southernmost part of the Maricunga Belt. Ore resources in the deposit total 900 million tonnes, containing 5.67×10^6 kg of gold (Muntean 1998).

We report here on the composition of grains of native gold and electrum, recovered from the Cerro Casale gold-rich porphyry system. Samples were taken from a broad vertical range and from different associated alteration-induced assemblages, lithologies and styles of mineralization. Considering that gold precipitated during two different stages of hydrothermal mineralization (potassic and white mica), we attempt to relate the geochemical behavior of gold with respect to types of

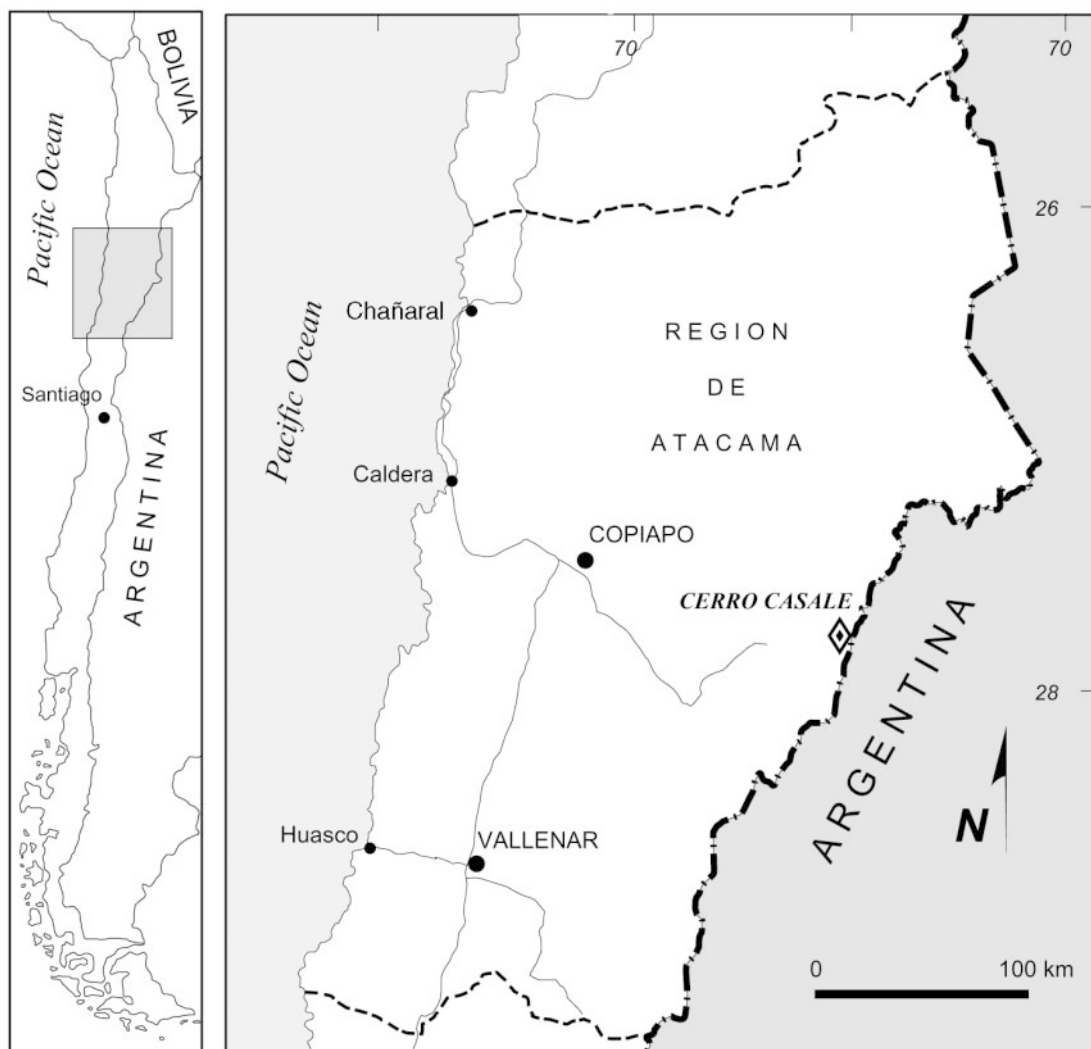


FIG. 1. Location map of the Cerro Casale ore deposit, in northern Chile.

hydrothermal alteration, styles of mineralization and types of host rock within the porphyry system.

GOLD MINERALIZATION IN THE MARICUNGA BELT

The Maricunga Belt hosts one of the largest concentrations of precious metals in the Andes. The Belt is related to andesitic to dacitic Upper Oligocene and Miocene volcanism and subvolcanic plutonism of the southern end of the Central Volcanic Zone of the Andes (Mpodozis *et al.* 1995, Kay *et al.* 1999). A number of precious metal epithermal and porphyry-related deposits occur between 26° and 28°S latitude and 69° to 69°30'W longitude. In the N–S-trending Belt, there are at least 10 major stratovolcanoes and many smaller domes, lava flows, and pyroclastic flow and fall deposits. Most of the stratovolcanoes exhibit large areas of acid-sulfate alteration that locally host epithermal gold and silver mineralization. Gold-rich porphyries occur within the eroded volcanic edifices (Vila & Sillitoe 1991, Sillitoe *et al.* 1991). Volcanic activity started at a number of places along the 200 km Maricunga Belt in late Oligocene time and continued until late Miocene time (26 to about 5 Ma). No specific areal pattern appears in age distribution of the Miocene volcanic rocks within the Belt (McKee *et al.* 1994), but two overlapping longitudinal subbelts of deposits were recognized by Sillitoe *et al.* (1991). The western is of latest Oligocene to early Miocene age (25–20 Ma), and the eastern is of middle Miocene age (14–12.5 Ma).

THE CERRO CASALE GOLD-RICH PORPHYRY

Geology

The Cerro Casale porphyry deposit is exposed in the eastern flank of the deeply eroded volcanic edifice of the Cadillal – Yeguas Heladas volcano complex. K–Ar ages of the volcanic rocks range between 14.7 and 13.4 Ma (Mpodozis *et al.* 1995). A K–Ar alunite age of 13.5 Ma was reported by Sillitoe *et al.* (1991) for the argillic cap at Cerro Catedral west of Cerro Casale deposit. Additional K–Ar whole-rock ages of these altered rocks of 14.6 ± 1.6 and 12.9 ± 0.6 Ma were reported by Mpodozis *et al.* (1995). More precise $^{40}\text{Ar}/^{39}\text{Ar}$ dating of a drill-core sample from Cerro Casale by Muntean (1998) yielded a plateau age of 13.89 ± 0.04 Ma based on biotite and a plateau age of 13.91 ± 0.04 Ma based on alunite from a quartz–alunite veinlet west of Cerro Casale.

The subvolcanic intrusive center at Cerro Casale is funnel-shaped, largely composed of medium-grained hornblende–biotite quartz diorite and biotite granodiorite porphyry (Fig. 2). The late porphyry is finer grained and commonly has more quartz phenocrysts than the early quartz diorite (Muntean 1998). The porphyry complex intruded early to middle Miocene volcanic rocks that reach a thickness of about 600 m and comprise dacitic to andesitic lavas, tuffs, and breccias with thin intercalations of felsic ignimbrite and sandstone (Vila & Sillitoe 1991). The granodiorite porphyry brecciated

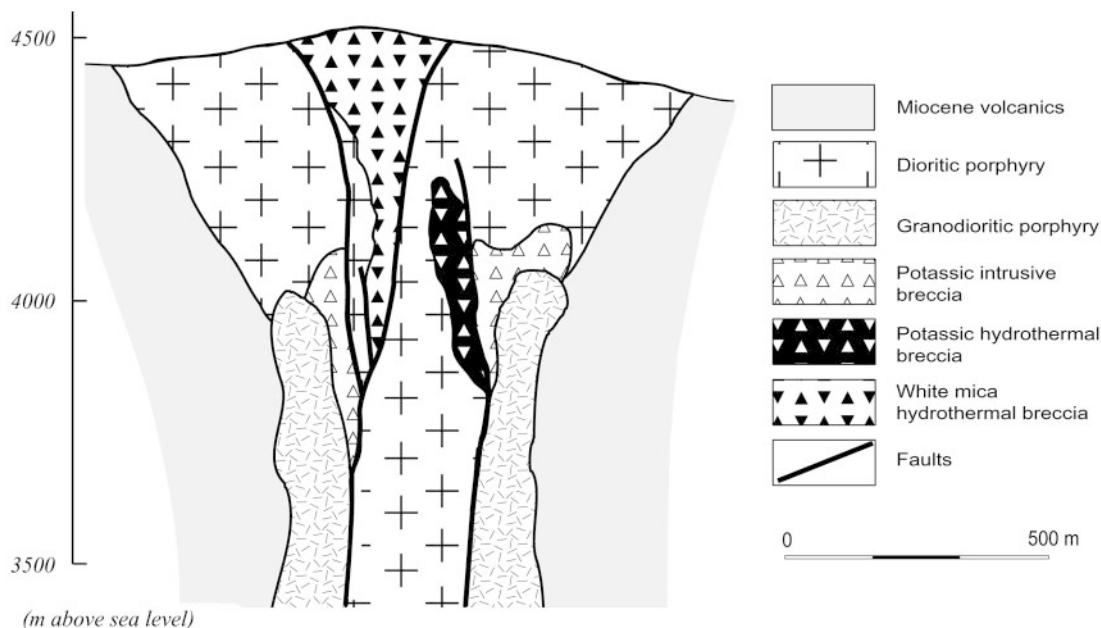


FIG. 2. Generalized geological cross-section of the Cerro Casale gold-rich porphyry.

the earlier-emplaced bodies of quartz diorite porphyry mainly along their roofs, forming intrusive breccias that contain subrounded to angular fragments of both porphyries and volcanic host-rocks (1 cm to 5 m). The matrix of the intrusive breccia consists of intensively altered granodioritic material.

Hydrothermal alteration and mineralization

The following summary description of the Cerro Casale orebody is based on the findings of Vila & Sillitoe (1991), Muntean (1998), Rivas (1999) and Sepúlveda (1999). The orebody (Fig. 2) is pipe-like and has a vertical extent of more than 1,000 m, with a roughly circular section, and a radius of about 250 m. Average gold contents are 0.9 ppm Au, and copper concentrations range between 0.15 to 0.30 wt%. Silver concentrations are low and range between 0.5 and 4 ppm (Sillitoe 1993).

Two broad types of hypogene alteration are associated with gold mineralization: a first stage of potassic alteration, and a late stage of white mica alteration. i) Potassic alteration leads to the assemblage biotite, K-feldspar, magnetite, hematite and quartz, with minor chalcocopyrite, tourmaline, bornite, and anhydrite. Vertical pipes of early hydrothermal and intrusive breccias are common. The breccia fragments correspond mainly to mineralized porphyries, and the matrix is dominated by minerals of the potassic assemblage. In the diorite and granodiorite porphyries and volcanic rocks, alteration and ore minerals occur as veinlets and disseminations. This assemblage is associated with a widespread quartz-dominant stockwork, which also contains biotite, magnetite, hematite and minor gold, chalcocopyrite, K-feldspar and tourmaline (A veinlets of Muntean 1988). Fluid-inclusion studies on hydrothermal quartz of the gold-bearing stockwork reveal homogenization temperatures from 495° to 565°C and salinities ranging between 20 and 70% NaCl equivalent (Muntean 1998). Gold grains (5 to 50 µm) occur mainly within quartz and occasionally as inclusions in magnetite. A zone of propylitic alteration, consisting of disseminations and veinlets of quartz, chlorite, white mica, pyrite, and epidote, forms an envelope around the nucleus of potassic alteration. ii) White mica alteration overprints the potassic assemblage. It is represented by veinlets and disseminations of quartz, white mica, pyrite, chalcocopyrite and gold (D veinlets of Muntean 1988). The Cu-sulfide is most abundant in the upper part of the deposit. During white mica alteration, a second stage of mineralized hydrothermal breccias developed in the orebody. Fragments correspond to mineralized blocks of both types of porphyry, with strong white mica alteration, cemented by barite, quartz, white mica, enargite, tennantite, chalcocopyrite, pyrite and gold. Gold occurs as 5 to 20 µm blebs in quartz, and occasionally within pyrite crystals. Fluid inclusions in quartz from this late episode of alteration show homogenization temperatures

from 200° to 300°C and salinities from 6 to 15% NaCl equivalent (Cuitiño *et al.* 1999).

SAMPLING AND ANALYTICAL TECHNIQUES

A total of 29 samples representing both types of porphyry, magmatic and hydrothermal breccias and volcanic host-rock were collected from diamond drill-cores at various depths. From these samples, a total of 176 grains of native gold (>10 µm) were recovered, from quartz stockwork in potassic alteration zones and from white mica veinlets, and from the matrix of hydrothermal breccias. Gold grains were observed in each sample; before separation by hand-picking, a detailed description of alteration types, lithology and related mineralization was done.

The chemical analyses were done with a CAMECA electron microprobe equipped with a Tracor Northern operating system at the Université Paul Sabatier, in Toulouse, for six elements (Fe, Cu, As, Ag, Au, Bi) using wavelength-dispersion spectrometry (WDS). For most runs, an accelerating voltage of 20 kV was used, with a beam current of 25 to 30 nA and a spot size of approximately 2 µm. A ZAF program was used to correct all the analytical data on precious metals acquired with pure metal standards. Counting time was 20 seconds on standards and 30 seconds on the unknowns. All analyzed samples were examined by back-scattered electron imaging (BEI), and no significant compositional zoning was observed. Data quality was assessed by replications of analysis of sample and standard, indicating precision within the 95% confidence level, and accuracy within the 90% confidence level for only Au, Ag and Cu. Other elements were either not within these set confidence-levels or were undetected, and hence have been omitted from further interpretation and discussion.

RESULTS

Table 1 presents analytical results for all grains of native gold, indicating the sample number (keyed into Fig. 2), host rock-type, associated type of alteration, style of mineralization, and elevation. The gold crystals deposited during potassic alteration present high abundances in Ag (8 to 27 wt.%: Fig. 3) and low concentrations of Cu (not detected to 0.23 wt.%: Fig. 4). However, the composition of the gold crystals related to the early stage of the hydrothermal activity differs in the granodiorite and diorite porphyries; gold crystals recovered from the granodiorite porphyry that represents the center of the hydrothermal system have higher abundances in Ag (17 to 27 wt.%) and lower concentrations in Cu (not detected to 0.07 wt.%); gold crystals recovered from the diorite porphyry exhibit between 8 to 17 wt.% Ag and up to 0.23 wt.% Cu.

The gold crystals deposited during the white mica alteration contain the lowest range of Ag concentrations

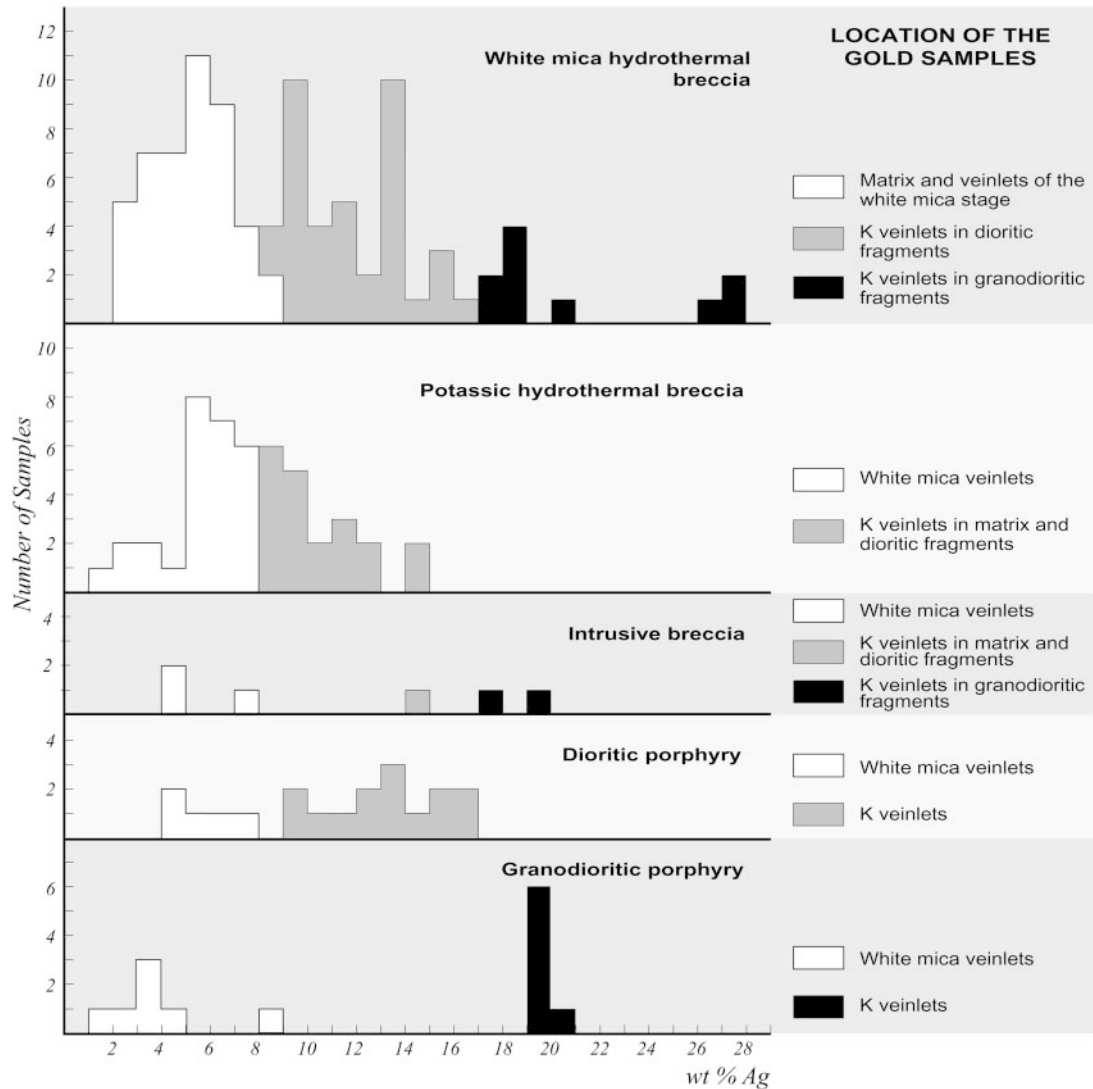


FIG. 3. Silver concentration in gold crystals from the Cerro Casale porphyry.

(1 to 9 wt.%) and relatively high concentrations in Cu (0.06 to 0.34 wt.%). Furthermore, the gold crystals recovered from fragments of both types of porphyry included in the white mica hydrothermal breccia maintain their original Ag and Cu composition.

Gold in potassic alteration exhibits the lowest fineness, 1,000 Au/(Au + Ag), ranging from 730 to 825 in the granodiorite porphyry, and from 832 to 920 in the diorite porphyry (Fig. 5). In contrast, the gold crystals in the white mica zone show the highest fineness, varying between 914 and 982.

DISCUSSION

Potassic alteration in Cerro Casale is mainly restricted to intrusive rocks, in which veinlets contain coexisting hypersaline brine and vapor-rich inclusions that indicate of temperatures homogenization above 500°C (Muntean 1998). These types of fluids are widely believed to be of magmatic origin. Magmatic and hydrothermal brecciation and widespread stockwork at Cerro Casale indicate that magmatic fluids boiled probably shortly after leaving the melt. At this stage, most of the dissolved gold will partition along with chloride

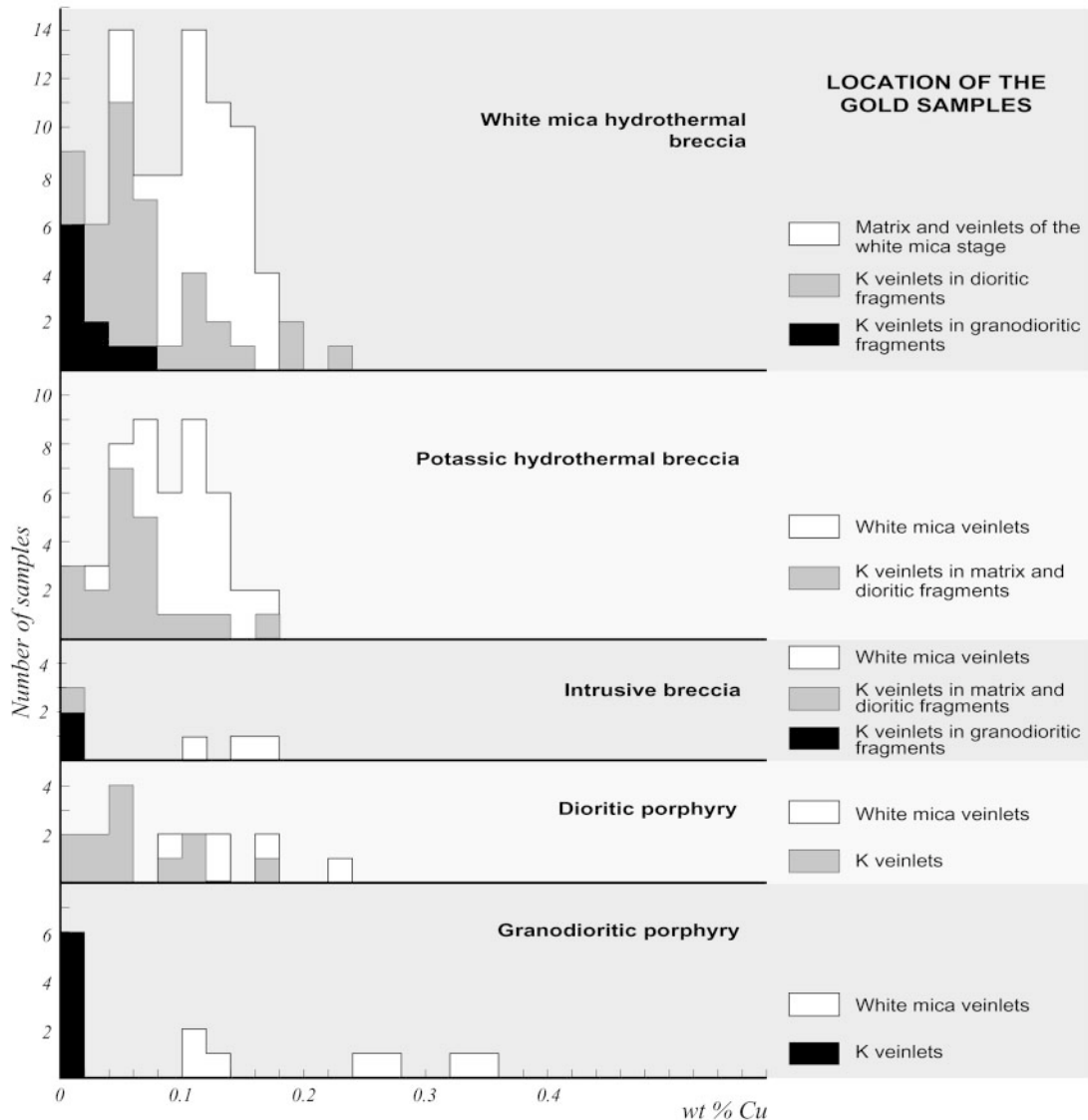


FIG. 4. Copper concentration in gold crystals from the Cerro Casale porphyry.

into the brine phase (Gammons & Williams-Jones 1997). This gold-bearing high-density fluid will tend to infiltrate the parent intrusion, forming the deposit along with potassic alteration. The scarcity of sulfides and the abundance of hematite and magnetite in the early alteration-induced assemblage likely reflect the oxidized nature of the initial fluids. Considering that Au and Ag solubilities at high-temperature and oxidized conditions are due to chloride complexes (Gammons & Williams-Jones 1997, Arancibia & Clark 1996, Huston *et al.* 1992, Shikazono & Shimizu 1987), the precious metals may

precipitate as Ag-rich gold crystals. In hydrothermal fluids where chloride complexes are the dominant transporting agent for Au and Ag, the composition of the native Au is largely controlled by temperature; differences in solubility between gold and silver both increase with a drop of temperature (Gammons & Williams-Jones 1995). Hydrothermal systems initiated at high oxygen fugacities would, given the availability of the ore metals, therefore, have the inherent potential both to concentrate Au and inhibit Cu deposition (Arancibia & Clark 1996). Candela *et al.* (1996) reported experi-

Host	Type and location of gold	Elevation m	Cu wt%	Ag wt%	Au wt%	Fineness	#
White mica	WM (matrix)	4,022	0.05-0.18	2.42-8.68	92.3-99.4	914-977	37
		3,858	<i>0.12</i>	<i>4.99</i>	<i>95.89</i>	<i>951</i>	
hydro-thermal breccia	WM (veinlet in PD frag.)	3,915	0.12-0.16	3.03-7.42	92.9-98.4	926-970	6
		3,865	<i>0.14</i>	<i>5.42</i>	<i>95.35</i>	<i>945</i>	
breccia	K (veinlet in PD frag.)	4,022	n.d.-0.23	8.02-16.91	83.5-92.6	832-920	34
		3,858		<i>11.89</i>	<i>86.70</i>	<i>882</i>	
	K (veinlet in PGD frag.)	3,944	n.d.-0.07	17.27-27.06	73.2-83.9	730-829	10
		3,859		<i>21.02</i>	<i>79.72</i>	<i>791</i>	
Potassic hydro-thermal breccia	WM (veinlet in matrix)	3,968	0.04-0.17	1.85-7.94	92.8-99.8	921-982	27
		3,850	<i>0.11</i>	<i>5.73</i>	<i>95.30</i>	<i>943</i>	
	K (matrix)	3,924	n.d.-0.18	8.33-12.25	88.3-93.4	877-918	11
		3,850		<i>9.88</i>	<i>91.25</i>	<i>902</i>	
	K (veinlet in PD frag.)	3,968	n.d.-0.14	8.49-14.60	87.0-92.0	856-915	10
		3,850		<i>10.79</i>	<i>90.02</i>	<i>893</i>	
Igneous breccia	WM (veinlet in matrix)	3,863	0.12-0.18	4.72-7.71	93.1-95.3	924-953	3
			<i>0.15</i>	<i>5.73</i>	<i>93.90</i>	<i>943</i>	
	K (veinlet in PD frag.)	3,887	0.02	14.36	86.6	858	1
		3,887	0.02-0.03	17.93-19.01	81.7-83.0	811-822	2
			<i>0.03</i>	<i>18.47</i>	<i>82.35</i>	<i>817</i>	
Andesite	WM (veinlet in andesite)	3,370	0.24-0.30	4.00-4.25	96.6-97.3	958-960	3
			<i>0.27</i>	<i>4.13</i>	<i>97.00</i>	<i>959</i>	
Diorite porphyry	WM (veinlet in PD)	3,885	0.09-0.23	4.21-7.06	93.0-96.7	929-958	5
		3,669	<i>0.15</i>	<i>5.52</i>	<i>95.12</i>	<i>948</i>	
	K (veinlet in PD)	3,887	n.d.-0.18	9.57-16.85	82.4-91.1	832-904	14
		3,669		<i>13.17</i>	<i>87.48</i>	<i>869</i>	
Grano-diorite porphyry	WM (veinlet in PGD)	3,912	0.11-0.33	1.80-8.28	92.6-98.7	918-982	7
		3,330	<i>0.22</i>	<i>3.83</i>	<i>96.69</i>	<i>962</i>	
	K (veinlet in PGD)	3,395	n.d.-0.01	19.48-20.83	78.8-82.0	791-808	6
				<i>19.95</i>	<i>81.00</i>	<i>802</i>	

WM (matrix): Gold crystals within matrix of white mica hydrothermal breccia.

WM (veinlet in PD frag.): Gold crystals in white mica veinlet from diorite porphyry fragment within hydrothermal breccia.

WM (veinlet in matrix): Gold crystals in white mica veinlet cross-cutting matrix from potassic hydrothermal breccia.

WM (veinlet in andesite): Gold crystals in white mica veinlet from andesitic host-rock.

WM (veinlet in PD): Gold crystals in white mica veinlet within diorite porphyry.

WM (veinlet in PGD): Gold crystals in white mica veinlet from granodiorite porphyry.

K (veinlet in PD frag.): Gold crystals in potassic veinlet from diorite porphyry fragment within hydrothermal breccia.

K (veinlet in PGD frag.): Gold crystals in potassic veinlet from granodiorite porphyry fragment within hydrothermal breccia.

K (matrix): Gold crystals within potassic matrix of hydrothermal breccia.

K (veinlet in PD): Gold crystals in potassic veinlet within diorite porphyry.

K (veinlet in PGD): Gold crystals in potassic veinlet from granodiorite porphyry.

Number of gold grains analyzed. Average values are shown in italics.

The full dataset can be ordered from the Depository of Unpublished Data, CISTI, National Research Council, Ottawa, Ontario K1A 0S2, Canada.

mental data indicating that the partition coefficient for gold from a silicic melt into a supercritical aqueous phase is about five times greater than that for copper. These data suggest that the earliest exsolved fluids should have the highest Au:Cu ratio. If crystallization continues, the melt should be rapidly depleted in gold, and later fluids should have a lower Au:Cu ratio. Thus, for mineralization associated with a given intrusion, the Au:Cu ratio should increase inward and downward in the deposit, reflecting the observed distribution of gold compositions during potassic alteration at Cerro Casale.

The modeling by Gammons & Williams-Jones (1997) suggests that during boiling, most of the H₂O and H₂S will partition into the vapor phase. On account of the temperature drop, the vapor may condense into a low-salinity, H₂S-rich liquid of mixed magmatic and meteoric heritage. This liquid will tend to sink and recirculate throughout the early mineralized porphyry, producing white mica alteration. Retrograde boiling of this fluid, as revealed by late hydrothermal brecciation, led to the second-stage precipitation of gold. The abundance of sulfides in the white mica assemblage suggests a fluid in which aqueous sulfur occurs dominantly as sulfide, and gold is transported as bisulfide complexes. These fluids precipitate forming Ag-poor and Cu-rich gold crystals. Fluid-inclusion data on late hydrothermal quartz indicate temperatures between 200° and 300°C. Experimental data at these temperatures show that solubilities of Ag and Cu occur as bisulfide complexes (Crerar & Barnes 1976, Gammons & Williams-Jones 1997, Xiao *et al.* 1998, Mountain & Seward 1998). However, Huston *et al.* (1992) and Gammons & Williams-Jones (1995) reported that Ag exhibits great stability as chloride complex at temperatures of 300°C and less for a wide range of Cl concentrations. These differences in the transport mechanism can explain the Ag-poor and Cu-rich gold crystals that precipitate during the late stage of alteration. Considering that Cerro Casale exhibits very low abundances of Ag, the limited availability of Ag in the hydrothermal fluids in equilibrium with white mica can also account for the Ag-poor gold crystals.

At the Cerro Casale deposit, the gold crystals maintain their original composition in fragments of both porphyries included in the white mica hydrothermal breccia. This suggests that: i) during the late stage of alteration, the gold that precipitated during potassic alteration was not dissolved and retransported, and ii) the fluids that produced the late stage of alteration themselves carried a second input of gold, probably of magmatic origin.

Unfortunately, there are few reports of Au, Ag and Cu concentrations in gold crystals, relating their geochemical behavior with stages of hydrothermal mineralization and types of host rocks within the orebody, in epithermal and porphyry deposits.

In spite of this limitation, we compare in Figure 6 the composition of gold in the Cerro Casale deposit with: i) the El Guanaco high-sulfidation epithermal orebody, northern Chile (Ulloa 2001; 9 samples), ii) the Pimenton low-sulfidation epithermal deposit, central Chile (Ulloa 2001, 11 samples), iii) the low- and high-sulfidation epithermal deposits of Bolivia (Ulloa 2001, 249 samples), iv) the Santo Tomas II gold-rich porphyry copper in the Philippines (Tarkian & Koopman 1995; 10 samples), in which gold deposition is related to potassic alteration, and v) the Grasberg gold-rich porphyry copper in Indonesia (Rubin & Kile 1997; 11 samples) with gold related to silicic alteration.

Lithology and Type of Gold

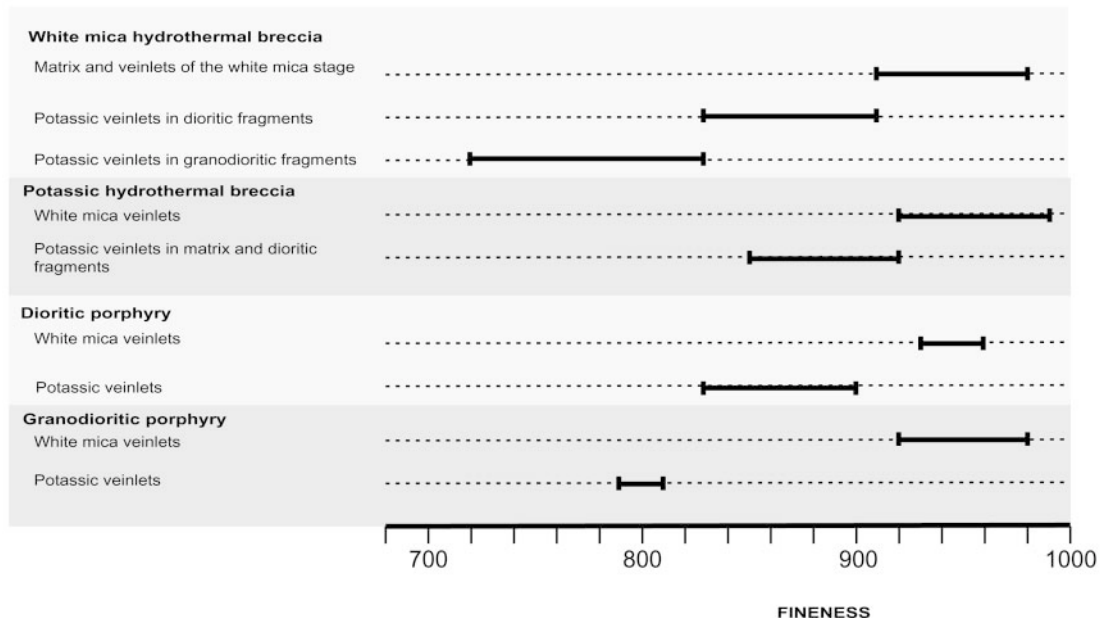


FIG. 5. Fineness values of the gold samples studied.

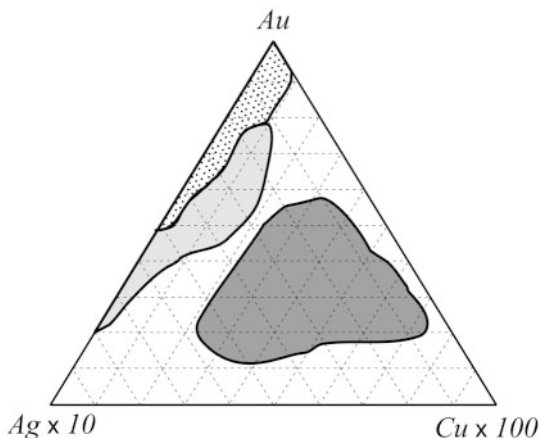


FIG. 6. Au–Ag–Cu discrimination diagram for gold deposited in epithermal deposits (dotted), the Cerro Casale gold porphyry (light grey), and gold-rich copper porphyries (dark grey).

In terms of the ternary system Au–Ag–Cu (Fig. 6), there are significant compositional differences in the gold crystals among the types of hydrothermal deposits. Gold from epithermal deposits is Cu-depleted and tends to be Au-rich. Gold from the Cerro Casale orebody

is also Cu-depleted and tend to be richer in Ag in comparison to epithermal gold crystals, and exhibits a tendency of increasing Cu-content with more Au enrichment. Gold crystals from gold-rich copper porphyries show the highest Cu concentrations, defining an area that is well distinguished from the other two types of gold-bearing ore deposits.

The Au–Ag–Cu diagram shows that the composition of gold from epithermal, gold-porphyry, and gold-rich porphyry-copper deposits differs. Although more research is needed, it seems that the composition of gold precipitated may help in the discrimination among gold-bearing hydrothermal deposits.

ACKNOWLEDGEMENTS

This study was financed by the Grants FONDEF 1033 from CONICYT, Chile. The work presented here is based on the M.Sc. theses of FS and PR, which were supported by Placer Dome. We thank the invaluable comments and suggestions of the referees, Robert F. Martin and James R. Craig.

REFERENCES

- ARANCIBIA, O.N. & CLARK, A.H. (1996): Early magnetite – amphibole – plagioclase alteration-mineralization in the Island Copper porphyry copper – gold – molybdenum deposit, British Columbia. *Econ. Geol.* **91**, 402-438.

- CANDELA, P.A., PICCOLI, P.M. & WILLIAMS, T.J. (1996): Preliminary study of gold partitioning in sulfur-free, high oxygen fugacity melt/volatile phase system. *Geol. Soc. Am., Abstr. Programs* **28**, A-402.
- CRERAR, D.A. & BARNES, H.L. (1976): Ore solution geochemistry. V. Solubilities of chalcopyrite and chalcocite assemblages in hydrothermal solutions at 200° to 350°C. *Econ. Geol.* **71**, 772-794.
- CUITIÑO, L., VIVALLO, W. & CORNEJO, C. (1999): Microtermometría de inclusiones fluidas en el depósito de Au-Cu Cerro Casale, Maricunga, Chile. *Proc. XIV Geol. Congress of Argentina* **2**, 352-353.
- GAMMONS, C.H. & WILLIAMS-JONES, A.E. (1995): Hydrothermal geochemistry of electrum: thermodynamic constraints. *Econ. Geol.* **90**, 420-432.
- _____ & _____ (1997): Chemical mobility of gold in the porphyry-epithermal environment. *Econ. Geol.* **92**, 45-59.
- HUSTON, D.L., BOTRILL, R.S., CREELMAN, R.A., ZAW, K., RAMSDEN, T.R., RAND, S.W., GEMMEL, J.B., JABLONSKI, W., SIE, S. H. & LARGE, R.R. (1992): Geological and geochemical controls on the mineralogy and grain size of gold-bearing phases, Eastern Australian volcanic-hosted massive sulfide deposits. *Econ. Geol.* **87**, 512-563.
- KAY, S.M., MPODOZIS, C. & COIRA, B. (1999): Neogene magmatism, tectonism and mineral deposits of the central Andes (22° to 33° Latitude). In *Geology and Ore Deposits of the Central Andes* (B.J. Skinner, ed.). *Soc. Econ. Geol., Spec. Publ.* **7**, 27-59.
- McKEE, E.H., ROBINSON, A.C., RYTUBA, J.J., CUITIÑO, L. & MOSCOSO, R. (1994): Age and Sr isotopic composition of volcanic rocks in the Maricunga Belt, Chile: implications for magma sources. *J. S. Am. Earth Sci.* **7**, 167-177.
- MOUNTAIN, B.W. & SEWARD, T.M. (1998): The hydrosulphide/sulphide complexes of copper (I): experimental determination of stoichiometry and stability at 22°C and reassessment of high temperature data. *Geochim. Cosmochim. Acta* **63**, 11-29.
- MPODOZIS, C., CORNEJO, P., KAY, S.M. & TITTLER, A. (1995): La franja Maricunga: síntesis de la evolución del frente volcánico oligoceno-mioceno de la zona sur de los Andes Centrales. *Rev. Geol. Chile* **22**, 273-314.
- MUNTEAN, J.L. (1998): *Magmatic-Hydrothermal Gold Deposits of the Maricunga Belt, Northern Chile*. Ph.D. thesis, Stanford Univ., Stanford, California.
- RIVAS, P. (1999): *Geoquímica de cristales de oro del depósito Cerro Casale, Franja Maricunga, Norte de Chile*. M.Sc. thesis, Department of Geology, Univ. de Chile, Santiago, Chile.
- RUBIN, J.N. & KYLE, J.R. (1997): Precious metal mineralogy in porphyry, skarn and replacement type ore deposits of the Ertzberg (Gunung Bijih) district, Irian Java, Indonesia. *Econ. Geol.* **92**, 535-550.
- SEPÚLVEDA, F. (1999): *Control de las variables intensivas y termodinámicas de los fluidos hidrotermales en la composición química del oro en el depósito Cerro Casale, Norte de Chile*. M.Sc. thesis, Univ. de Chile, Santiago, Chile.
- SHIKAZONO, N. & SHIMIZU, M. (1987): The Ag/Au ratio of native gold and electrum and the geochemical environment of gold vein deposits in Japan. *Mineral. Deposita* **22**, 309-314.
- SILLITOE, R.H. (1993): Gold-rich porphyry copper deposits: geological model and exploration implications. In *Mineral Deposit Modeling* (R.V. Kirkham, W.D. Sinclair, R.I. Thorpe & J.M. Duke, eds.). *Geol. Assoc. Can., Spec. Pap.* **40**, 465-478.
- _____, McKEE, E.H. & VILA, T. (1991): Reconnaissance K-Ar geochronology of the Maricunga gold-silver belt, northern Chile. *Econ. Geol.* **86**, 1261-1270.
- TARKIAN, M. & KOOPMANN, G. (1995): Platinum-group minerals in the Santo Tomas II (Philex) porphyry copper-gold deposit, Luzon Island, Philippines. *Mineral. Deposita* **30**, 39-47.
- ULLOA, C. (2001): *Modelo de discriminación entre depósitos epitermales, mesotermiales y de pórfido basado en la geoquímica de cristales de oro*. M.Sc. thesis, Univ. de Chile, Santiago, Chile.
- VILA, T. & SILLITOE, R.H. (1991): Gold-rich porphyry systems in the Maricunga Belt, northern Chile. *Econ. Geol.* **86**, 1238-1260.
- XIAO, Z., GAMMONS, C.H. & WILLIAMS-JONES, A.E. (1998): Experimental study of copper (I) chloride complexes in hydrothermal solutions at 40° to 300°C and saturated water vapor pressure. *Geochim. Cosmochim. Acta* **40**, 1329-1341.

Received October 9, 2000, revised manuscript accepted March 20, 2001.